

# Capacitance-based assessment of water content in lubricating oils for marine engines

## ARTICLE INFO

Received: 25 March 2025  
 Revised: 26 April 2025  
 Accepted: 5 May 2025  
 Available online: 29 May 2025

*This article presents a method for assessing the water content in lubricating oils used in Navy ship marine engines, based on capacitance measurements. The method uses the dependence of capacitance on the permeability of the dielectric, which changes with water content and temperature. Real-time measurements are carried out using the Arduino Mega 2560 platform on samples with known water content. Experimental results show characteristic changes in capacitance and hysteresis effect due to water evaporation during heating. The proposed solution provides an effective online tool for oil condition monitoring, enabling early detection of engine damage and optimization of maintenance.*

**Key words:** *marine diesel combustion engine, Arduino Mega 2560, dielectric analysis of lubricating oils, fault diagnosis of marine engines, water contamination*

This is an open access article under the CC BY license (<http://creativecommons.org/licenses/by/4.0/>)

## 1. Introduction

One of the primary causes of piston damage in internal combustion engines is the deterioration of the physicochemical properties of lubricating oil, which leads to the rupture of the oil film. Consequently, both mixed and dry friction phenomena occur, resulting in tribological damage to the engine's friction interfaces [8, 10, 19]. An example of such damage is shown in Fig. 1.



Fig. 1. Friction traces on the inner liner of the plain bearing

During engine operation, the physicochemical properties of the lubricating oil change, among which the most critical for engine reliability are:

- viscosity
- total base number
- total acid number
- flash point
- oxidation resistance and thermal stability
- lubricity
- the ability to wash away and disperse contaminants
- the ability to separate water.

Changes in the oil parameters typically occur gradually, following the curve shown in Fig. 2. The plotted curve

denotes the functional dependence of the parameter on the measurement conditions. Its gradient may assume positive or negative values, indicating that, depending on the underlying physical sensitivity, the parameter can either increase or decrease as the conditions vary [14, 21].

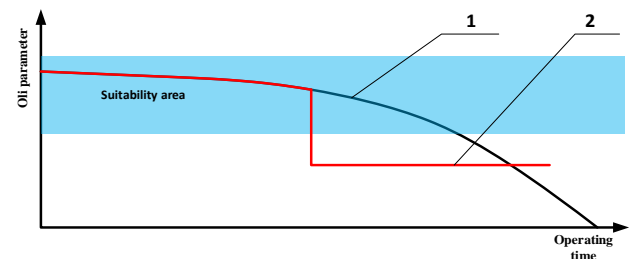


Fig. 2. An exemplary curve illustrating the change in an oil parameter as a function of its service time: 1 – natural degradation of oil parameters 2 – sudden change in oil parameters resulting from damage

In most cases, during engine operation, changes in the physicochemical parameters of lubricating oil occur in accordance with curve no. 1 and are predictable. Based on this, oils are utilized following a strategy that specifies a determined operating time (in line with the recommendations of both engine and oil manufacturers). Moreover, during the operation of marine engines, periodic inspections of the physicochemical parameters of the oils are conducted in specialized laboratories. This strategy generally prevents damage caused by the deterioration of the oil's physicochemical properties [15, 21].

However, there are instances during operation when the physicochemical parameters of the oils change suddenly in an unpredictable manner (contrary to the adopted strategy). Such a scenario is illustrated by curve no. 2 shown in Fig. 2. The most common cause of a sudden change in the oil's physicochemical parameters is engine damage, which results in the contamination of the oil with solid particles – usually metallic in nature (originating from its friction nodes) – as well as water or fuel. Contamination with fuel

is typically accompanied by a decrease in viscosity and a reduction in flash point. Contamination with water, on the other hand, is accompanied by a rapid increase in oil density (in extreme cases, the oil transforms into an emulsion with a paste-like consistency), which drastically deteriorates its lubricating properties. The source of water contamination during engine operation is the cooling system. In the case of marine reciprocating engines, the oil may be contaminated with fresh water, which is primarily used to cool the cylinder liners and engine heads, or with water containing salt ions (seawater) employed to cool the turbocharged air and, occasionally, the lubricating oil [10, 14, 18].

From the perspective of piston engine operation, the early detection of both water contamination in the oil and oil contamination in the cooling water is of critical importance. During engine operation, the oil is subjected to a higher pressure than the cooling water. Consequently, in the event of a leak, oil is expected to enter the cooling water, whereas during engine downtime, the likelihood of water infiltrating the oil increases. Therefore, it is essential to develop an online detection method capable of identifying both water in the oil and oil in the cooling water [9, 11–13]. This task has been undertaken by a research team from the Institute of Ship Construction and Operation of the Naval Academy.

The proposed method is based on the use of a slot capacitor, in which the dielectric is provided by the lubricating oil (in the case of detecting water in oil) or by the cooling water (in the case of detecting oil in water). According to Equation 1, the capacitance of the capacitor depends directly on the plate surface area ( $S$ ), the distance between the plates ( $d$ ), and the relative permittivity ( $\epsilon_0$ ) of the dielectric between the plates. For the capacitor, the values of the plate separation and surface area are fixed and characteristic of its design, while the independent variable is the relative permittivity of the dielectric (i.e., the oil–water mixture) [3, 8, 18].

$$C = \epsilon_0 \cdot \epsilon_r \cdot \frac{S}{d} \quad (1)$$

## 2. Method assumptions

It is widely accepted that the oils used on ships are dielectrics whose dielectric properties may change during operation [2, 4, 15, 16, 20]. One source of these changes is the natural aging process of the oil (oxidation), during which the hydrocarbons in the oil are converted into esters with polar structures. During operation, the oil may become contaminated with solid particles, fresh water, or seawater. Both the oil's aging processes and its contamination with water (especially seawater) lead to changes in its dielectric properties. It is assumed that the relative permittivity of oil,  $\epsilon$ , is approximately 2.5, whereas that of fresh water is close to 80. In the case of seawater, the relative permittivity is several times higher due to the presence of salt ions from elements such as sodium, magnesium, calcium, and potassium. It should be noted that the relative permittivity is highly dependent on temperature; for example, in distilled water it varies from 88 to 55.3 as the temperature changes from 0 to 100°C, as illustrated in Fig. 3.



Fig. 3. The influence of water temperature on its relative electrical permittivity

In the case of oil contaminated with water, it can be assumed that the relative electric permittivity of the oil–water mixture is proportional to the relative water content (Fig. 4).

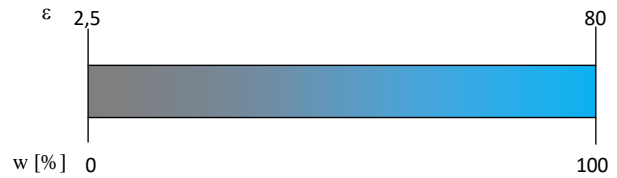


Fig. 4. The likely dependence of relative permittivity as a function of water content in oil

Direct determination of the relative permittivity is impossible. Therefore, indirect methods are typically used. The most common approach utilizes the dependence of the capacitance of a parallel-plate capacitor (Eq. 1). To determine the theoretical value of the relative electrical permittivity of mixtures, a linear or nearly linear model is usually employed, as described by the following relationship [1, 3, 21]:

$$\epsilon_r(w) = \epsilon_{r,oil} + k \cdot w \quad (2)$$

where:  $\epsilon_{r,oil}$  – the relative permittivity of pure oil (without water),  $w$  – the water content (e.g., in ppm or %),  $k$  – the calibration coefficient quantifying the influence of water content on the permittivity.

In practical studies, the sensor (capacitor) must be calibrated by measuring its capacitance for oil samples with known water content, and on that basis, a correction function is derived:

$$C(w) = C_0 + a_1 w + a_2 w^2 + \dots \quad (3)$$

In order to determine the coefficients  $C_0$  and  $a_1$ , capacitance measurements are performed for various known values of water content,  $w_i$ . Then, using the least squares method, the model parameters are determined [1, 3, 21]:

$$\begin{bmatrix} C_1 \\ C_2 \\ \vdots \\ C_n \end{bmatrix} = \begin{bmatrix} 1 & w_1 \\ 1 & w_2 \\ \vdots & \vdots \\ 1 & w_3 \end{bmatrix} \begin{bmatrix} C_0 \\ a_1 \end{bmatrix} \quad (4)$$

The solution is:

$$\begin{bmatrix} C_0 \\ a_1 \end{bmatrix} = (W^T W)^{-1} W^T C \quad (5)$$

where  $w$  is the matrix of water content, and  $C$  is the vector of measured capacitances.

In the conducted research, various methods for measuring the capacitance of a capacitor were considered, ranging

from utilizing the resonance phenomenon of currents and voltages in RLC circuits to determining the time constant of a capacitor-resistor circuit with known capacitance [1, 3, 21].

The first method examined was based on the resonance phenomenon in RLC circuits, where the capacitor, with the oil or water under investigation serving as the dielectric, represents the capacitance  $C$ . In practice, either series or parallel resonance is employed, with elements such as the capacitor, inductor, and resistor connected either in series (Fig. 5a) or in parallel (Fig. 5b) [1, 3, 17, 21]:

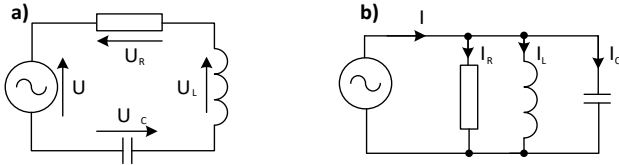


Fig. 5. RLC resonance circuit: a) series, b) parallel

In the case of the series resonance circuit (Fig. 5a), voltage resonance occurs, which in practice means that the amplitude of the voltage across the individual passive components  $U_L$ ,  $U_R$ , and  $U_C$  reaches its maximum when the resonance phenomenon occurs. The voltage across the passive elements is described by the following relationship [1, 3, 21]:

$$U_L = I \cdot L \cdot \omega_r = \frac{U}{R} \cdot \sqrt{\frac{L}{C}} \quad (6)$$

At the resonant frequency, the voltage across the inductor and the capacitor is described by the following relationship:

$$|U_L| = -|U_C| \quad (7)$$

Conversely, the resonant frequency is determined according to the following expression:

$$f_r = \frac{1}{2 \cdot \pi \cdot \sqrt{LC}} \quad (8)$$

In situations where the objective is to determine the capacitor's capacitance, the source frequency must be adjusted so that the voltage across the passive components is maximized. The resonant frequency is thereby a function of the capacitor's capacitance.

In the case of a parallel resonance circuit (Fig. 5b), the phenomenon is termed current resonance. The principle for determining the capacitor's capacitance is fundamentally analogous to that employed in the series resonance scenario. However, a key difference from a measurement perspective is that the circuit current is monitored, and the generator frequency at which this current reaches its maximum is identified. The resonant frequency in a parallel RLC circuit is described by the following relationship [1, 3, 21]:

$$f_r = \frac{R}{\sqrt{L}} \sqrt{C} \quad (9)$$

The resonant frequency value is also a function of the capacitor's capacitance. The methods described for determining the capacitor's capacitance (which is a function of the dielectric permittivity of the insulator) can be successfully employed in the construction of a measurement system. However, the drawbacks of such a measurement system include the duration of the measurement process and the need to utilize a sinusoidal voltage generator with an adjustable frequency. The measurement time is influenced by the necessity to scan a wide frequency range, which is both problematic and time-consuming in practice. Consequently, the authors have opted for an alternative method for measuring the capacitor's capacitance. They decided to construct a measurement system based on determining the time constant of a circuit composed of a capacitor and a resistor with a known resistance. The RC circuit time constant is defined as the time required for the voltage measured across the capacitor to reach 63.2% of its fully charged voltage. The capacitor's capacitance in the RC circuit is related to the time constant according to the following relationship [1, 3, 10, 19, 21]:

$$T_C = R \cdot C \quad (10)$$

Based on Equation 10, the capacitor's capacitance was calculated:

$$C = \frac{T_C}{R} \quad (11)$$

A graphical illustration of the principle of determining the capacitor's capacitance based on the RC circuit's time constant is shown in Fig. 6.

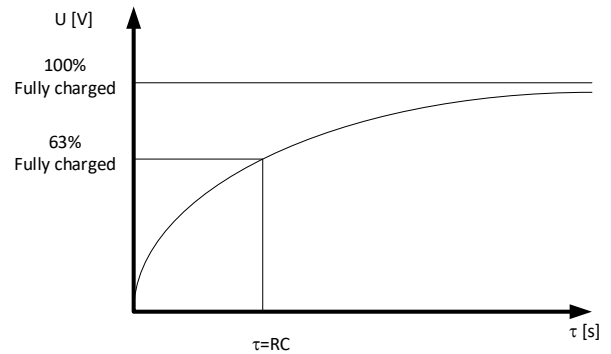


Fig. 6. Illustration of the principle for determining the time constant of an RC circuit

The constructed measurement system is based on the Arduino Mega 2560 microcontroller. This system enables the measurement of the charging time of a capacitor connected in series with a resistor (which reduces the charging current and, consequently, increases the circuit's time constant). This approach enhances the accuracy of the time measurement (i.e., the number of microcontroller clock cycles), thereby improving the precision of the capacitor's capacitance determination. In the conducted studies, two types of capacitors were utilized, both employing oil with variable water content as the dielectric. A slot capacitor and a specially fabricated cylindrical capacitor were used for

this purpose. An illustration of the measurement system employing the slot capacitor is shown in Fig. 7.

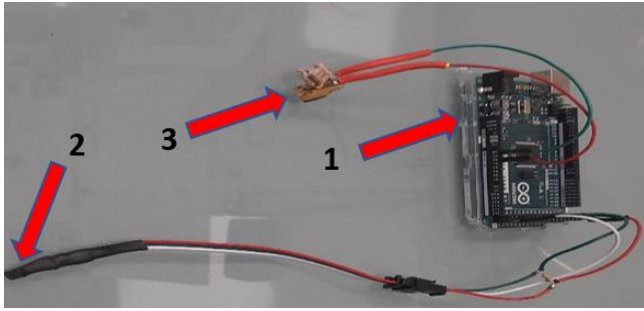


Fig. 7. Measurement system used in the studies: 1 – Arduino Mega 2560 microcontroller, 2 – slot capacitor, 3 – 18B20 temperature sensor

Additionally, the measurement system has been equipped with an 18B20 temperature sensor, which enables real-time monitoring of the temperature of the investigated medium. Temperature measurement is critical because there is a dependency between the temperature of the liquid (the dielectric of the liquid capacitor) and its capacitance. This relationship is characterized by the temperature capacitance coefficient  $T_{WC}$  [1, 3, 21]:

$$T_{WC} = \frac{1}{C} \cdot \frac{\delta C}{\delta T} \quad (12)$$

Conversely, the impact of temperature is delineated by the following relationship:

$$C(T) = C(T_0) \cdot [1 + T_{WC} \cdot (T - T_0)] \quad (13)$$

### 3. Research plan

The foundation of this research is the development of a method for detecting engine damage that results in the mixing of lubricating oil with cooling water. It is essential to measure the water content in the lubricating oil as well as the oil content in the cooling water, and the proposed method must support real-time (online) measurements.

It was determined that the optimal approach would be to measure the electrical capacitance of a capacitor, whose dielectric is constituted by the lubricating oil and cooling water under investigation. According to Eq. (1) and (13), the capacitance of the capacitor is a function of its temperature and the relative dielectric constant of the insulator forming the gap between its electrodes. The capacitance value depends on the oil temperature (see Fig. 3) and its water content (see Fig. 4). The geometric properties of the capacitor are assumed to remain constant throughout the experiments (thermal expansion of its components is neglected).

Experimental investigations were carried out by measuring the capacitance of a slot capacitor (immersed in the test liquid) as a function of water content and temperature. For this purpose, an apparatus based on the Arduino Mega 2560 platform was developed, enabling continuous measurement and transmission of both the capacitor's capacitance and the liquid's temperature to a computer. The measurements are performed with a sampling frequency of 1 Hz and a resolution of 12 bits.

During the experiment, the sample under investigation is placed on a magnetic stirrer equipped with a heating function. The sample contains the slot capacitor as well as a temperature sensor. Continuous measurements of temperature and capacitance are recorded while the sample is stirred and heated. The sample is heated from ambient temperature until it reaches 95°C – a value that approximates the standard operating temperature of lubricating oil in marine engines (80–95°C). Once the target temperature is attained, the heater is turned off. Measurements continue from the onset of heating until the sample cools back to ambient temperature (typically around 20°C). Additionally, samples are periodically collected and analyzed microscopically (see Fig. 8) to assess the homogeneity of the mixture [5, 6].

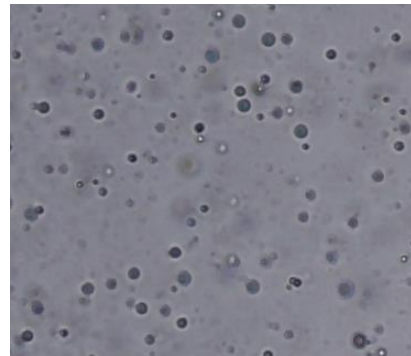


Fig. 8. Microscopic view of an oil sample with a water content of 0.5%

Under laboratory conditions, the water content in the sample decreases during measurement due to evaporation caused by heating. This is evidenced by the irreproducibility of the measurement results obtained during the heating and cooling phases of the sample. Furthermore, the foaming of the mixture's surface at elevated temperatures indicates the occurrence of water evaporation.

The study was conducted in accordance with a completely randomized statistical design. This design enables a more precise evaluation of the effect of a single factor – in this case, the water content in the oil – than would be possible using traditional statistical hypothesis testing. The investigated factor can assume values at each level  $p$ , limited solely by the technical conditions of the experiment. The null hypothesis, assumed a priori, postulates that the analyzed input factor has no effect on the output variable. A factor is deemed significant if the computed value of the test statistic is equal to or greater than the critical value specified in the relevant statistical tables. For a completely randomized design, it is most advantageous to use the Fisher-Snedecor F statistic [6, 7].

The planning matrix for the completely randomized statistical design, which is used to assess the impact of the single input factor on the output variable, is presented in Table 1.

The F test statistic is calculated according to the following relationship:

$$F = \frac{\sum_{i=0}^p n_i (\bar{y}_i - \bar{y})^2 (n - p)}{[\sum_{i=1}^p \sum_{j=1}^q n_{ij} (y_{ij} - \bar{y})^2 - \sum_{i=1}^p n_i (\bar{y}_i - \bar{y})^2] (p - 1)} \quad (14)$$

where:  $n_i$  – the number of measurements of the input factor at a given level,  $n$  – the total number of measurements,  $\bar{y}_i$  – the mean measurement result in the  $i$ -th row,  $\bar{y}$  – the overall mean of all measurement results,  $y_{ij}$  – denotes the value of the  $j$ -th output factor at level  $i$ ,  $p$  – the number of levels of the input factor variability.

Table 1. Planning Matrix for the Completely Randomized Statistical Design [6, 7]

Input factor level	Number of experiments		
	1	...	q
1	$y_{11}$	...	$y_{1q}$
$\vdots$	$\vdots$	$\vdots$	$\vdots$
p	$y_{p1}$	...	$y_{pq}$

The calculated F test statistic should be compared with the critical value determined from the table (for the chosen significance level  $\alpha$  and for the degrees of freedom for the numerator calculated according to the following relationship:

$$f_1 = f_1 = p - 1 \quad (15)$$

and for the denominator according to the formula:

$$f_2 = f_m = n - p \quad (16)$$

If the computed F value is greater than or equal to the critical value  $F_{kr} F \geq F_{kr} = F_{(\alpha; f_1; f_2)}$ , the effect of the investigated factor is deemed significant. Conversely, if  $F \leq F_{kr}$ , this indicates that within the examined range of variability, the input factor does not influence the output variable [6, 7].

In the experimental studies, measurements were conducted over mass concentrations of water in oil at 0%, 0.5%, and 1%. All experiments were repeated five times, which facilitated a comprehensive statistical analysis of the results.

#### 4. Results

As a result of the conducted studies, the capacitance values of a capacitor immersed in the test sample were obtained as a function of the mass fraction of water in the oil. The empirical results are presented graphically, illustrating the recorded variation in the capacitor's capacitance as a function of temperature (ranging from 80°C to 100°C, which corresponds to the typical operating temperature of the oil) for different water mass fractions (Fig. 9). Each plot displays the results of five experiments (for each concentration), as indicated by the colors of the data points. In Figure 9, for water concentrations of 0.5% and 1%, a characteristic hysteresis loop is observed, evidenced by the non-overlapping data points recorded during the heating and cooling phases of the mixture. This behavior is attributed to the water evaporation process, which consequently alters the sample composition. Therefore, only the data corresponding to the heating phase were used for further analysis. Due to water evaporation, a new sample with a predetermined water content was required for each repetition of the measurement at a given concentration.

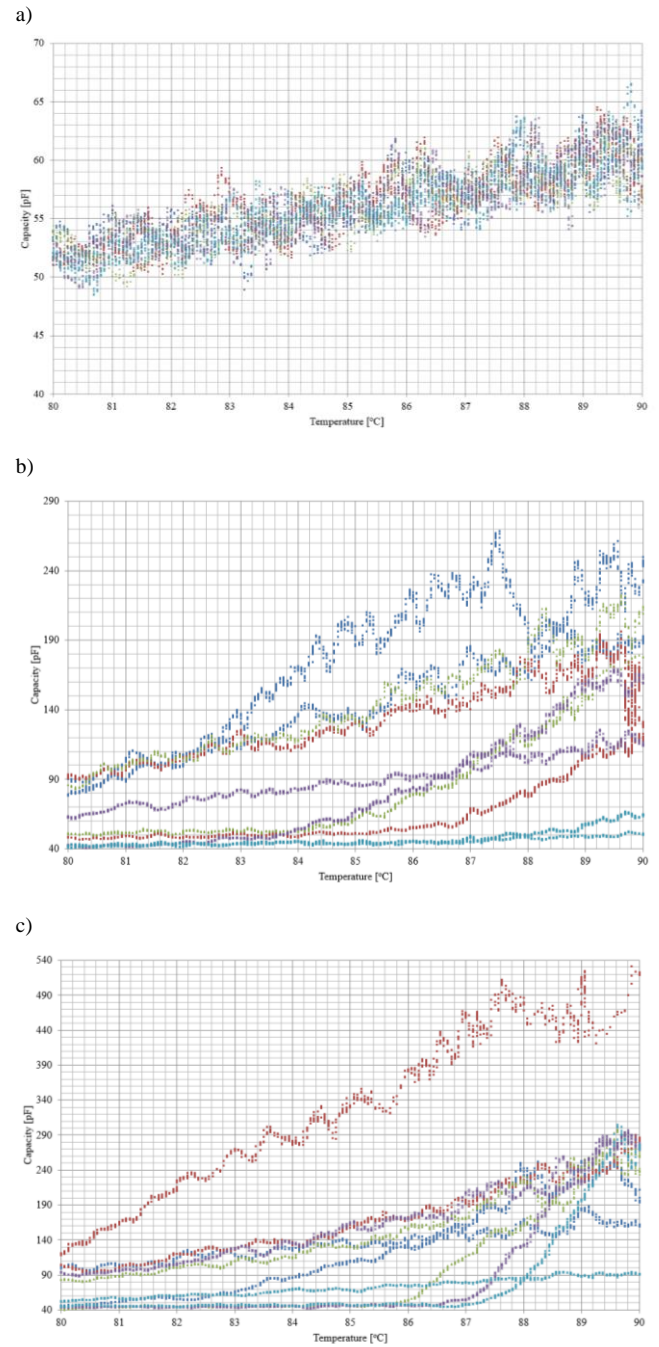


Fig. 9. Recorded capacitor capacitance curves as a function of the temperature of the oil-water mixture for the respective mass fractions: a) pure oil, b) 0.5% water, c) 1% water

Measurements were conducted with a constant time step of 1 Hz, so that the resulting data (temperature and capacitor capacitance) were functions of time. Consequently, it was necessary to derive capacitance curves as a function of the dielectric temperature. To this end, the measured capacitance values were averaged for each temperature value, with a resolution of 0.1°C. Subsequently, for each considered temperature (for each concentration), a single capacitance value was computed as the arithmetic mean of all five repeated measurements. The resulting data are presented in Fig. 10.

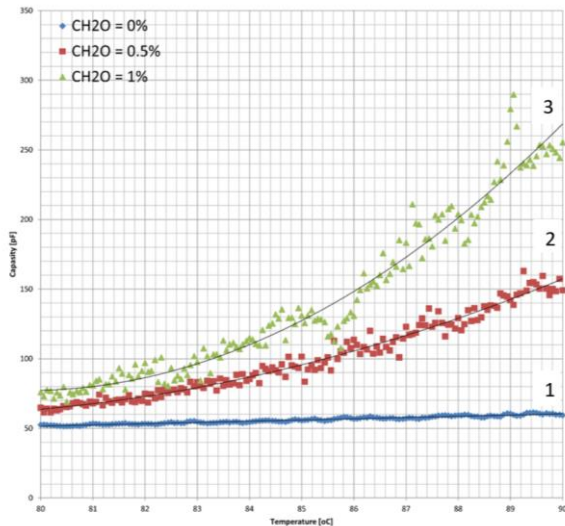


Fig. 10. Capacitance variation curves as a function of the dielectric temperature for the respective mass fractions of water in oil: 1 – oil, 2 – a mixture of 0.5% water and 99.5% oil, 3 – a mixture of 1% water and 99% oil

### 5. Conclusion

The conducted studies demonstrated that the proposed method for detecting and quantifying the mass fraction of water in engine oil is effective. It enables the real-time

(online) acquisition of clear information regarding engine damage that results in the contamination of lubricating oil with water. The developed method is sufficiently sensitive to allow operators to take measures that minimize – practically, to prevent – the occurrence of secondary damage stemming from the deterioration of the oil’s lubricating properties. Furthermore, by employing the capacitance-based approach, it is possible to detect metallic contaminants with a diameter equal to or greater than the distance between the capacitor plates. Such contamination will cause a short-circuit in the capacitor, which unequivocally indicates damage to the engine’s friction components.

A significant drawback of the proposed method is the necessity of obtaining a homogeneous mixture of water and oil. However, in the case of internal combustion engines, the oil is intensely mixed with any water present during operation.

The proposed method can also be utilized for detecting engine oil contamination in water and for determining the proportions of individual components in mixtures and emulsions of liquids with differing dielectric properties. Currently, the research team is investigating the determination of the mass fractions of oil in both seawater and freshwater, as well as the quantification of biocomponents in marine fuels.

### Nomenclature

C	electric capacitance, vector of measured capacitance values [F]	S	surface area of the capacitor plates [m <sup>2</sup> ]
C(T <sub>0</sub> )	capacitance of the capacitor at the initial temperature [F]	T	temperature [K]
d	distance between the capacitor plates [m]	T <sub>c</sub>	time constant of the RC circuit [s]
I	current [A]	T <sub>WC</sub>	temperature capacitance coefficient
k	calibration coefficient defining the influence of water content on capacitance [-]	U	electric voltage [V]
L	inductance [H]	W	mass concentration of water in the mixture [%]
R	resistance [Ω]	ε <sub>0</sub>	permittivity of free space [F/m]
		ε <sub>r</sub>	relative permittivity of the dielectric [F/m]
		ε <sub>r,oil</sub>	relative permittivity of pure oil [F/m]

### Bibliography

- [1] Hambley AR, Pułka AK. Wprowadzenie do elektroniki i elektrotechniki. T. 2: Systemy cyfrowe (in Polish). PWN. Warszawa 2023.
- [2] Eidi A. Fabricated electromechanical resonator sensor for liquid viscosity measurement. *Metrol Meas Syst.* 2023;30: 223-234. <https://doi.org/10.24425/mms.2023.144868>
- [3] Floyd TL, Buchla DM. Principles of electric circuits: conventional current. Tenth edition, global edition. Pearson Education Limited. Harlow 2022.
- [4] Gomółka L, Augustynowicz A. Evaluation of applicability of dielectric constant in monitoring aging processes in engine oils. *Eksploata Niezawodn.* 2019;21(2):177-185. <https://doi.org/10.17531/ein.2019.2.1>
- [5] Idros MFM, Hashim H, Islam S, Ali SH. Capability of optical approach in condition based monitoring of lubricant oil. *Sensors and Transducers.* 2012;17:125-134. [https://sensorsportal.com/HTML/ST\\_JOURNAL/PDF\\_Files/P\\_SI\\_272.pdf](https://sensorsportal.com/HTML/ST_JOURNAL/PDF_Files/P_SI_272.pdf)
- [6] Kokot F, Hyla-Klekt L, Kokot S. Badania laboratoryjne: zakres norm i interpretacja (in Polish). Wyd. 5 uakt. i rozsz. Wydawnictwo Lekarskie PZWL. Warszawa 2011.
- [7] Korzyński M. Metodyka eksperymentu: planowanie, realizacja i statystyczne opracowanie wyników eksperymentów technologicznych (in Polish). Wydawnictwa Naukowo-Techniczne. Warszawa 2006.
- [8] Kozak M. A comparison of thermogravimetric characteristics of fresh and used engine oils. *Combustion Engines.* 2019;178(3):289-292. <https://doi.org/10.19206/CE-2019-350>
- [9] Kozak M, Siejka P. Soot contamination of engine oil – the case of a small turbocharged spark-ignition engine. *Combustion Engines.* 2020;182(3):28-32. <https://doi.org/10.19206/CE-2020-305>
- [10] Macián V, Tormos B, Olmeda P, Montoro L. Analytical approach to wear rate determination for internal combustion engine condition monitoring based on oil analysis. *Tribol Int.* 2003;36(10):771-776. [https://doi.org/10.1016/S0301-679X\(03\)00060-4](https://doi.org/10.1016/S0301-679X(03)00060-4)
- [11] Malinowska M, Zera D. The oil engine lubricity variation analysis of engine oil applied in Cegielski-Sulzer motor 3AL25/30. *Zeszyty Naukowe Akademii Morskiej w Gdyni.* 2016;96:93-104. <https://sj.umg.edu.pl/artukul-466.html>

- [12] Molenda J, Wolak A, Zajac G, Cieloch P, Chudy D. Assessment of the suitability of paper chromatography for quick diagnostics of the operating condition of engine oil. *Ekspluat Niezawodn.* 2023;25(2):162912. <https://doi.org/10.17531/ein/162912>
- [13] Olszewski W. The possibility of estimate quality state of using motor oil by measuring dielectrical properties. *Journal of Kones.* 2001;8(3-4). <https://yadda.icm.edu.pl/baztech/element/bwmeta1.element.baztech-article-BUJ7-0005-0011>
- [14] Shinde H, Bewoor A. Analyzing the relationship between the deterioration of engine oil in terms of change in viscosity, conductivity and transmittance. 2017 International Conference on Advances in Mechanical, Industrial, Automation and Management Systems (AMIAMS). <https://doi.org/10.1109/AMIAMS.2017.8069185>
- [15] Shinde H, Bewoor A. Capacitive sensor for engine oil deterioration measurement. *AIP Conf. Proc.* 2018;1943:020099. <https://doi.org/10.1063/1.5029675>
- [16] Shinde HM, Bewoor AK, Kumar R, Elsheikh, Singh DV, Shanmugan S et al. Engine oil quality deterioration estimation using an integrated sensory system. *Proc Inst Mech Eng Part E J Process Mech Eng.* 2023;237(6):2257-2267. <https://doi.org/10.1177/09544089221135629>
- [17] Wolak A, Zajac G, Kumbár W. Evaluation of engine oil foaming tendency under urban driving conditions. *Ekspluat Niezawodn.* 2018;20(2):229-235. <https://doi.org/10.17531/ein.2018.2.07>
- [18] Zhang Z, Ouyang W, Liang X, Yan X, Yuan C, Zhou X et al. Review of the evolution and prevention of friction, wear, and noise for water-lubricated bearings used in ships. *Fric-tion.* 2024;12(1):1-38. <https://doi.org/10.1007/s40544-022-0707-5>
- [19] Zhou F, Yang K, Wang L. The effect of water content on engine oil monitoring based on physical and chemical indicators. *Sensors.* 2024;24(4):1289. <https://doi.org/10.3390/s24041289>
- [20] Zhu Q. Nonlinear systems: dynamics, control, optimization and applications to the science and engineering. *Mathematics.* 2022;10:4837. <https://doi.org/10.3390/math10244837>
- [21] Żółtowski B, Ćwik Z. *Leksykon diagnostyki technicznej* (in Polish). ATR. Bydgoszcz 1996.

Prof. Marcin Zacharewicz, DSc., DEng. – Faculty of Mechanical and Electrical Engineering, Polish Naval Academy, Poland.  
e-mail: [m.zacharewicz@amw.gdynia.pl](mailto:m.zacharewicz@amw.gdynia.pl)



Paweł Socik, MEng. – Faculty of Mechanical and Electrical Engineering, Polish Naval Academy, Poland.  
e-mail: [p.socik@amw.gdynia.pl](mailto:p.socik@amw.gdynia.pl)



Artur Bogdanowicz, DEng. – Faculty of Mechanical and Electrical Engineering, Polish Naval Academy, Poland.  
e-mail: [a.bogdanowicz@amw.gdynia.pl](mailto:a.bogdanowicz@amw.gdynia.pl)

